J. Fluid Mech. (1983), vol. 133, pp. 37–46
Printed in Great Britain

The turbulent recirculating flow field in a coreless induction furnace, a comparison of theoretical predictions with measurements

By N. EL-KADDAH AND J. SZEKELY

Department of Materials Science and Engineering, Massachusetts Institute of Technology, Cambridge, Massachusetts 02139

(Received 12 April 1982 and in revised form 28 February 1983)

A mathematical representation has been developed for the electromagnetic force field and the fluid-flow field in a coreless induction furnace. The fluid flow field was represented by writing the axisymmetric turbulent Navier–Stokes equations, containing the electromagnetic body-force term. The electromagnetic body force field was calculated by using a technique of mutual inductances. The k-ϵ model was employed for evaluating the turbulent viscosity, and the resultant differential equations were solved numerically.

The theoretically predicted velocity fields were in reasonably good agreement with the experimental measurements reported by Hunt & Moore; furthermore, the agreement regarding the turbulence intensities was essentially quantitative. These results indicate the k-ϵ model does provide a good engineering representation of the turbulent recirculating flows occurring in induction furnaces. At this stage it is not clear whether the discrepancies between measurements and the predictions, which were not very great in any case, are attributable either to the model or to the measurement techniques employed.

1. Introduction

In recent years there has been a growing interest in the development of an improved basic understanding of heat- and fluid-flow phenomena in coreless induction furnaces. The main motivation for this interest is essentially twofold. First, the actual operation of coreless induction furnaces as means for scrap melting and the refining of molten metals depends critically on the turbulent heat- and fluid-flow phenomena in this system. The second, more fundamental, motivation is that the turbulent recirculating fluid-flow phenomena in this system represent a very interesting class of electromagnetically driven flow problems.

Figure 1 shows a sketch of a typical coreless induction furnace, where it is seen that this consists of a refractory (or non-magnetic) crucible, containing a conducting metallic melt. The outer wall of the crucible is surrounded by water-cooled induction coils (connected as a single-phase or multiphase arrangement) through which a current is passed. The passage of this current through the coil in turn induces a current in the melt, and the interaction of this induced current with the associated magnetic field results in an electromagnetic force field, or Lorentz force field, which causes a recirculating motion of the melt.

The quantitative representation of this system has two essential components:

(1) the electromagnetic force field has to be calculated;

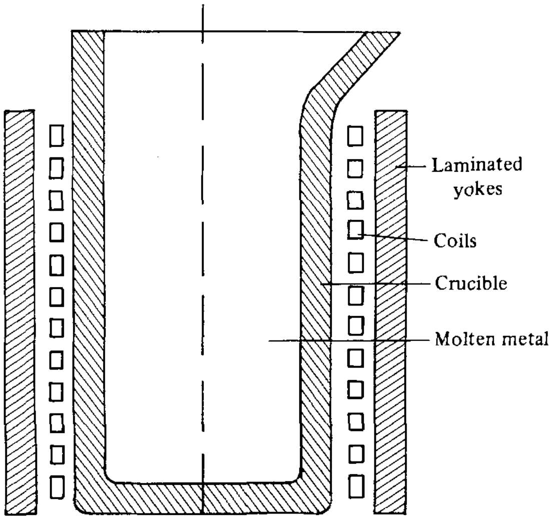

FIGURE 1. Sketch of an induction furnace.

(2) knowing the distributed body-force field, the fluid-flow field may then be obtained.

The following general observations may be appropriate at this stage.

When the magnetic Reynolds number is small the rate at which the electromagnetic field propagates is much faster than the fluid velocity; thus the force field and the fluid-flow field calculations may be uncoupled.

The calculation of the electromagnetic force field resulting from a given coil configuration is a classical problem in electrodynamics, which may be be readily accomplished using analytical techniques for simple geometries (Panofsky & Phillips 1955; Jackson 1962), or numerical procedures, e.g. the technique of mutual inductances for more complex systems.

If the flow is laminar, in principle the velocity field could be readily calculated by combining the known body forces field with the laminar Navier–Stokes equations (Hughes & Young 1966). However, this procedure is not readily applicable in the vast majority of practical cases, where the magnitude of the force field and the linear dimensions of the system result in a turbulent flow. The presence of turbulence precludes the use of simple analytical techniques. The approaches that have been devised to tackle problems of this type may be divided into two major groups.

(*A*) Starting with the rigorous form of the turbulent Navier–Stokes equations, order-of-magnitude approximations may be made for the various terms; thus approximate expressions may be deduced for the mean values of the various flow parameters (Szekely & Chang 1977*a*, *b*; Khaletzky 1976; Moore & Hunt 1982*a*).

(*B*) An alternative, engineering, approach that has been developed (Szekely & Chang 1977*a*, *b*; Szekely & Nakanishi 1975; Tarapore and Evans 1976, 1977) employed various turbulence models such as the k-W and the k-ϵ models to represent the Reynolds stresses, and thus obtained detailed maps of both the velocity fields and of the turbulence parameters.

Both these approaches have advantages and drawbacks. The technique of Hunt & Moore (1982*a*) is certainly elegant and provides a useful insight into relationships between the key system parameters. However, because of the approximations involved, the model cannot be used to predict the detailed velocity field, the maps of the turbulence, and thus cannot but provide very preliminary order-of-magnitude estimates regarding the key heat- and mass-transfer and dispersion phenomena that are of primary interest in the solution of practical engineering problems. The numerical approaches that have been developed for tackling problems of this type are certainly attractive because they are capable of addressing the very questions of practical interest, such as local shear rates, dispersion rates and ultimately the transport-controlled reaction kinetics (Szekely & Nakanishi 1975; Gosman *et al.* 1969; Launder & Spalding 1974; Launder 1976; Nakanishi *et al.* 1975).

The main drawbacks of these engineering calculations include the substantial computational labour required and the lack of a fundamental basis for the turbulence models employed. In view of the great potential usefulness of these techniques, it would be highly desirable to develop a critical comparison of these theoretical predictions with experimental measurements.

Up to the present only a limited range of such measurements has been available. Many of these involved the determination of surface velocities and tracer-dispersion rates; while the agreement between predictions and the measured data was quite good, auguring well for many engineering applications, a really rigorous test of these models has not been possible because of the lack of sufficiently accurate measurements. The recently published measurements of Moore & Hunt (1982*a*), kindly given to us prior to formal publication, using an inductively stirred mercury system, should provide a useful basis for a more rigorous test of the model. The purpose of this paper is to report on such an assessment.

2. Experimental

The experimental measurements have been reported by Moore & Hunt, and therefore only a very brief recapitulation will be given here.

A schematic sketch of the experimental arrangement is shown in figure 2. In essence the apparatus consisted of a water-cooled stainless-steel vessel approximately 0.3 m in diameter and 0.4 m high, containing mercury. Agitation was provided by an induction coil containing 11 uniformly spaced turns. The r.m.s. coil current was 1900 A, having a frequency of 50 Hz.

The actual measurements taken included the determination of the electromagnetic force field, using search coils and the measurement of both the time-smoothed and the fluctuating velocities, using a mechanical probe. This mechanical probe consisted of a perforated spherical shell made of tantalum, and the velocities were deduced from the drag exerted on this sphere. Measurements close to tank wall were made with a 'wall probe' described by Moore (1982).

3. The analysis

The analytical problem is to calculate the electromagnetic force field and the turbulent fluid-flow field in a cylindrical system, agitated by a symmetrically placed induction coil.

3.1. *Calculation of the electromagnetic force field*

The electromagnetic force field is given by

$$\boldsymbol{F} = \boldsymbol{J} \times \boldsymbol{B}, \tag{1}$$

where $\boldsymbol{J}$ is the induced current density and $\boldsymbol{B}$ is the magnetic flux density.

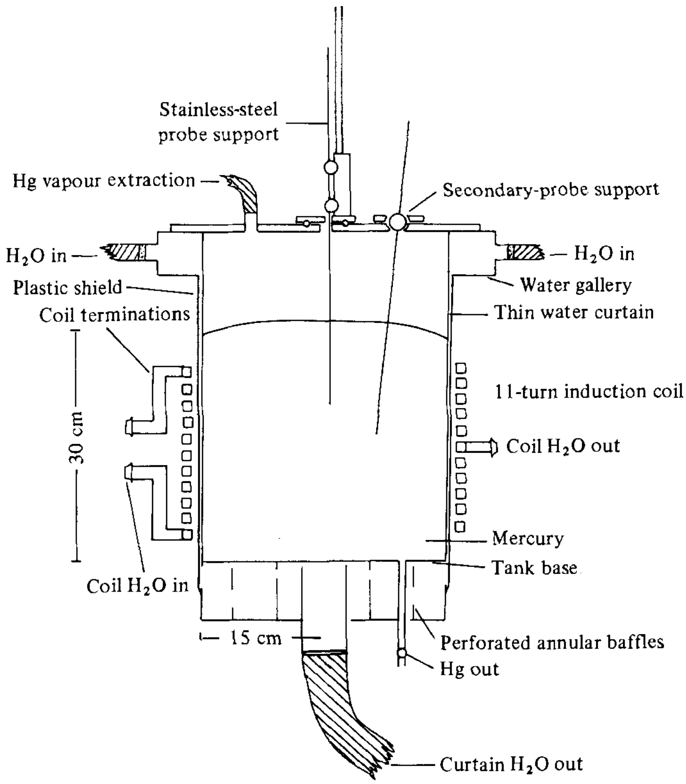

FIGURE 2. Salient features of the apparatus.

Thus the problem is to calculate $\boldsymbol{J}$ and $\boldsymbol{B}$ for a given geometry and coil current.

For idealized systems, e.g. infinitely long cylinders, and a travelling wave, this task may be accomplished analytically, through the solution of Maxwell's equations (Hughes & Young 1966). However, for the present system, an alternative technique, employing the concept of mutual inductances, is preferable.

For a cylindrical crucible, characterized by axial symmetry, the lines of equal current density are circles in planes perpendicular to the axis of the coil, i.e. the θ-direction. From Ampère's law the magnetic field in an elementary circuit in the melt may be written in terms of the vector potential $\boldsymbol{A}$ ($\boldsymbol{B} = \nabla \times \boldsymbol{A}$) as

$$A_\theta = \frac{m_0}{4\pi}\left\{\sum_{c=1}^{\text{melt}} (\boldsymbol{J}\cdot\boldsymbol{S})_c \oint \frac{\mathrm{d}l_s}{r'} + \sum_{k=1}^{\text{coil}} I(k) \oint \frac{\mathrm{d}l_k}{r'}\right\}, \tag{2}$$

where A_θ is the vector potential, $\mathrm{d}l$ is the line element of a circuit of constant current density and S is the cross-sectional area of the circuit. $I(k)$ is the coil current.

It should be noted that first term on the right-hand-side of (2) describes the induced potential, while the second term describes the applied potential.

From Faraday's law, the induced current in this circuit can be written for a time-harmonic field as

$$\oint J_i \, \mathrm{d}l_i = j\omega\sigma \left\{\sum_{c=1}^{\text{melt}} M_{i,c} (\boldsymbol{J}\cdot\boldsymbol{S})_i + \sum_{k=1}^{\text{coil}} M_{ik} I_{(k)}\right\}, \tag{3}$$

where

$$M_{i,c} = \frac{\mu_0}{4\pi} \oint \oint \frac{\mathrm{d}l_i \, \mathrm{d}l_c}{r'} \tag{4}$$

is the mutual inductance.

The calculation then proceeds by dividing the melt into elementary circuits (14 × 14 in the present case), each represented by (3), to be solved simultaneously, to obtain the induced current. Once the induced current field is known, the vector potential may be obtained from (2), which then allows the computation of the electromagnetic body-force field.

3.2. *Calculation of the fluid-flow field*

For cylindrical symmetry, the equations of continuity and motion take the following form:

equation of continuity

$$\frac{1}{r}\frac{\partial}{\partial r}(\rho r U_r) + \frac{\partial}{\partial z}(\rho U_z) = 0; \tag{5}$$

momentum balance in the z-direction

$$\frac{1}{r}\left[\frac{\partial}{\partial r}\left(\rho r U_r U_z\right)\right] + \frac{\partial}{\partial z}(\rho U_z^2) = -\frac{\partial p'}{\partial z} + \frac{1}{r}\frac{\partial}{\partial r}\left(r\mu_{\text{eff}}\frac{\partial U_z}{\partial r}\right) + 2\frac{\partial}{\partial z}\left(\mu_{\text{eff}}\frac{\partial U_z}{\partial z}\right) + \left[\frac{1}{r}\frac{\partial}{\partial r}\left(\mu_{\text{eff}}\, r\frac{\partial U_r}{\partial r}\right)\right] + \tfrac{1}{2}\mathrm{Re}\,(J_\theta B_r^*); \tag{6}$$

momentum balance in the r-direction

$$\frac{1}{r}\left[\frac{\partial}{\partial r}\left(\rho r U_r^2\right)\right] + \frac{\partial}{\partial z}(\rho U_r U_z) = -\frac{\partial p'}{\partial r} + \frac{2}{r}\frac{\partial}{\partial r}\left(r\mu_{\text{eff}}\frac{\partial U_r}{\partial r}\right) + \frac{\partial}{\partial z}\left(\mu_{\text{eff}}\frac{\partial U_r}{\partial z}\right) + \left[\frac{\partial}{\partial z}\left(\mu_{\text{eff}}\frac{\partial U_z}{\partial z}\right)\right] - \frac{2U_r\mu_{\text{eff}}}{r^2} + \tfrac{1}{2}\mathrm{Re}\,(J_\theta B_z^*). \tag{7}$$

Here the quantity μ_{eff} is the effective viscosity defined as

$$\mu_{\text{eff}} = \mu + \mu_{\text{t}}, \tag{8}$$

where μ_{t} may be estimated using the so-called k-ϵ model:

$$\mu_{\text{t}} = C_\mu \rho k^2/\epsilon. \tag{9}$$

Here k and ϵ are the turbulent kinetic energy and the turbulent kinetic-energy dissipation respectively.

Separate transport equations have to be written down for these, which take the following form:

$$\frac{\partial}{\partial z}(\rho U_z \phi) + \frac{1}{r}\frac{\partial}{\partial r}(\rho r U_r \phi) - \frac{\partial}{\partial z}\left(\frac{\mu_{\text{eff}}}{\sigma\phi}\frac{\partial \phi}{\partial z}\right) - \frac{\partial}{\partial r}\left(r\frac{\mu_{\text{eff}}}{\sigma\phi}\frac{\partial \phi}{\partial r}\right) = S_\phi, \tag{10}$$

where S_ϕ is the net rate of generation of turbulent properties per unit volume. The source terms S_k and S_ϵ in the transport equations for k and ϵ are given by

$$S_k = G - D, \tag{11}$$

$$S_\epsilon = \frac{C_1 \epsilon}{KG} - \frac{C_2 \rho \epsilon^2}{K}, \tag{12}$$

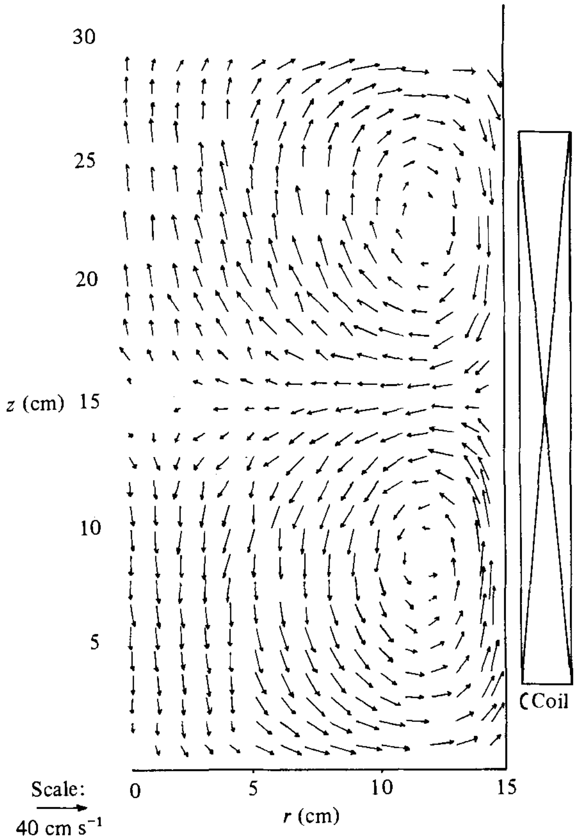

FIGURE 3. Experimentally measured velocity field for 1900 A coil current.

where

$$G = \mu_t\left[2\left\{\left(\frac{\partial U_z}{\partial z}\right)^2 + \left(\frac{\partial U_r}{\partial r}\right)^2 + \left(\frac{U_r}{r}\right)^2\right\} + \left(\frac{\partial U_z}{\partial r} + \frac{\partial U_r}{\partial z}\right)^2\right], \tag{13}$$

$$D = \rho\epsilon. \tag{14}$$

The values used for the constants, viz $C_\mu = 0.09$, $C_1 = 1.45$ and $C_2 = 1.92$, were taken from the work of Launder (1976) and Launder & Spalding (1974), and were not adjusted in any way in the course of the computation.

In principle, the boundary conditions, which are required to complete the statement of the problem, specify zero velocity at the solid surfaces, zero shear at the free surface and the existence of symmetry about the centreline. Furthermore, the quantities k and ϵ are set equal to zero at the solid surfaces and their gradients are stipulated to be zero at the free surfaces.

As a practical matter, in line with the procedures used for modelling turbulent flows, wall functions were used to define the shapes of these curves between the bounding surfaces and the nearest grid points to the wall (Launder & Spalding 1974). These wall functions were deduced from the universal velocity distribution for turbulent boundary layers without pressure-gradient and body forces, which represents an oversimplification. This is an area where careful experimental measurements could provide a useful refinement.

The governing equations were put in a finite-difference form, using a 16×16 grid,

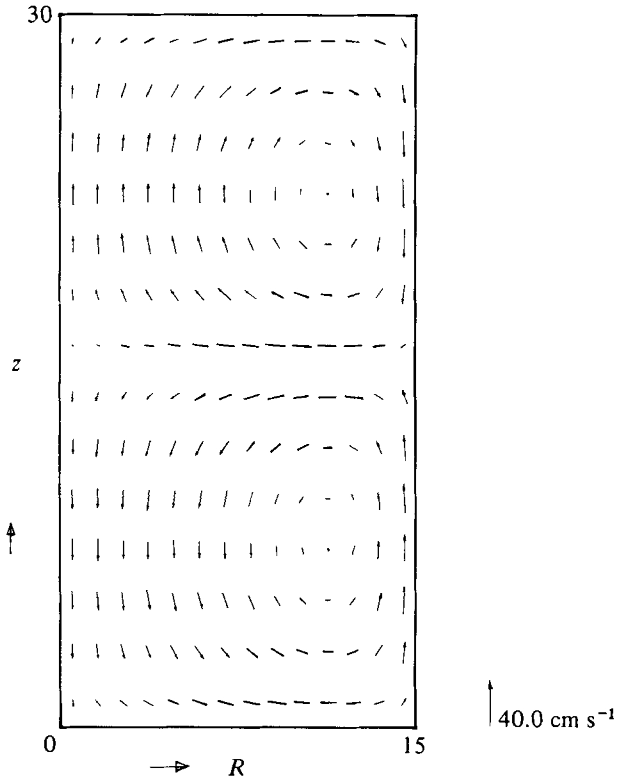

FIGURE 4. Computed velocity field for 1900 A coil current.

and the resultant set of simultaneous nonlinear algebraic equations was solved using an iterative technique. Typically the computer-time requirements were about 120 s on MIT's IBM 370 digital computer.

4. Comparison of the computed results with measurements

Since the principal concern here is a critical comparison of the experimentally measured and the theoretically predicted velocity fields and turbulence characteristics, the treatment presented will be confined to this aspect of the problem. Two sets of somewhat differing experimental measurements of the electromagnetic force field vector were also provided by Moore & Hunt, but a comparison of these with the model predictions was inconclusive. Since the technique of mutual inductances is well established and the experimental determination of the electromagnetic force field may have involved some inaccuracies, this apparent discrepancy was not pursued further.

Figures 3 and 4 show the experimentally measured and the theoretically predicted maps of the velocity vector. Quantitative agreement is seen regarding the nature of the flow and the position of the recirculating loops; furthermore, the numerical values of the velocity vector are comparable.

Figure 5 shows the experimentally measured profile of the axial velocity, determined at a vertical position, corresponding to the eye of the upper vortex. Also shown, with the broken line, is the computed velocity profile. It is seen that these two profiles are quite similar, with fairly good agreement regarding the absolute values, but that the two curves do not coincide. Whether this discrepancy is attributable either to

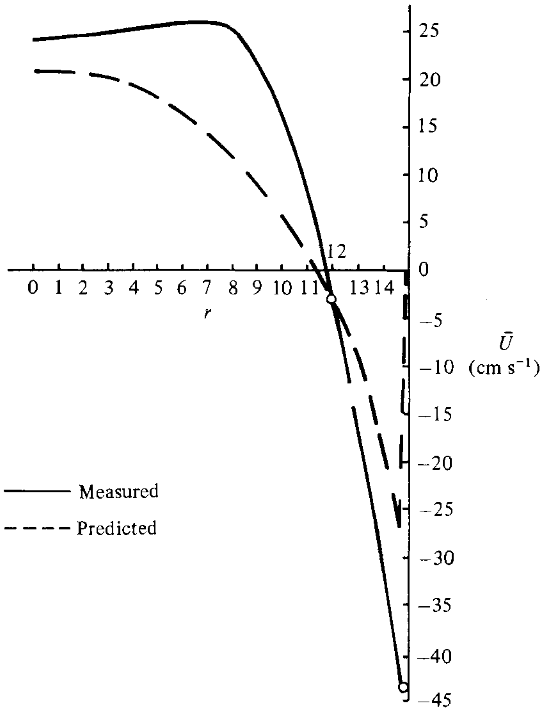

FIGURE 5

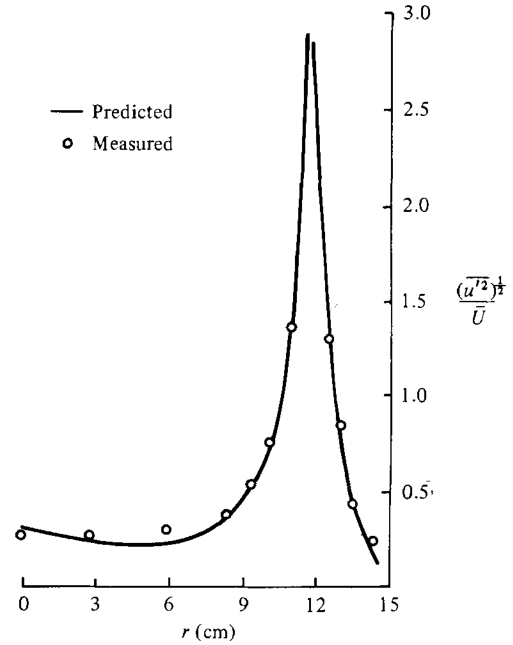

FIGURE 6

FIGURE 5. A comparison of the experimentally measured (full line) and theoretically predicted (broken line) radial variation of the axial velocity component at a height of 22.5 cm.

FIGURE 6. A comparison of the experimentally measured (circles) and the theoretically predicted (full line) radial profile of the turbulence intensity.

possible shortcomings of the model or to experimental errors will be discussed subsequently.

Figure 6 shows a plot of the local value of the turbulence intensity, as a function of the radial position. The measurements are given with the circles, while the theoretical predictions are designated by the full line. The agreement is seen to be very good, rather better than that found for the velocity profiles.

5. Discussion

A comparison is made between experimentally measured fluid-velocity profiles and profiles of the turbulence intensity as reported by Moore & Hunt for an inductively stirred mercury pool, and theoretical predictions based on mutual inductances and the two-equation k-ϵ model.

This comparison was thought to be instructive, because these measurements represent the most detailed data on inductively stirred systems available up to the present.

The principal findings of the work may be summarized as follows.

(1) The theoretical predictions regarding the general nature of the flow were found to be in very good agreement with the measurements.

(2) The profiles of the time-smoothed velocity near the wall were reasonably well

predicted by the model, although there were certain discrepancies, particularly at a large distance from the wall.

There was very good agreement between the measured and the predicted profiles of the turbulence intensities.

In discussing these results it is fair to say that important reservations must be expressed regarding the fundamental basis of the k-ϵ model and that of the wall functions. However, at present there appears to be no generally applicable alternative for doing engineering-type calculations for turbulent recirculating flows where details are required of the turbulence-energy distribution and of the local heat- or mass-transfer rates.

On the basis of information available in the literature, the use of this model has been quite successful in a number of instances, and the findings reported in this paper appear to support this contention.

On the basis of prior experience, one would expect turbulence models of the type employed here to predict the overall flow field rather well, because neither the particular features of the turbulence model employed nor the damping effect of the electromagnetic field on the turbulence are likely to be very important in the bulk. In the bulk of the fluid the convective transport of momentum is likely to dominate, thus the predictions for the overall circulation pattern are unlikely to be sensitive to the particular turbulence model employed. A much more critical test of the model would be provided by the assessment of the predictions in the near-wall region, and of the turbulence-energy distribution.

In considering the experimental technique employed, it has to be recognized that the characterization of electromagnetically driven turbulent recirculating flows is notoriously difficult, because of the problems inherent in the use of traditional measuring equipment. The technique employed by Moore & Hunt is thought to be ingenious, but perhaps not subjected to a lengthy enough testing period to eliminate all possible experimental errors. The relatively large size of the probe or even the alternative probing devices employed near the wall (compared to a standard hot film device) makes the reliability of the measurements in the very near wall regions somewhat problematic, where accurate data would be most desirable.

It follows that it is not really quite clear whether the discrepancies between measurements and predictions are uniquivocally attributable to the shortcomings of the model or to the measurement techniques.

While there was good agreement between the predicted and the experimentally measured velocity profiles, a certain discrepancy was evident, both in the immediate vicinity of the wall and in the bulk of the fluid.

It should be remarked that the experimentally obtained velocity profiles do not satisfy the equation of continuity, i.e.

$$\int_0^R U_z 2\pi \,\mathrm{d}r = 0; \tag{15}$$

thus some questions may be raised regarding the accuracy of the absolute values of the measured velocities. One may comment that the calibration curves for the probe were not exactly linear, which in conjunction with the straight-line relationship actually employed provided a significant error band, especially at low velocities. This should not be taken as a criticism of the experimental technique, because the problems of velocity measurements in liquid-metal systems are generally appreciated by workers in this field.

It is of interest to note the perhaps unexpectedly very good agreement between the theoretically predicted and the experimentally measured turbulence intensities. The k-ϵ model explicitly assumes local anisotropy, and serious questions may be raised as to whether this condition has been met in an inductively stirred system. One may speculate that some self-cancelling errors may have come into play; alternatively, perhaps, the experimental technique was not sensitive enough to pick up some of the higher harmonics. It should be remarked, furthermore, that the errors introduced due to the nonlinearity of the calibration curve will affect the absolute values of the velocity far more than the velocity ratios. Since the turbulence-intensity curves shown in figure 6 represent ratios, these would be less affected by calibration errors.

In conclusion one must state that, notwithstanding its shortcomings as far as lacking a fundamental basis, the k-ϵ model appears to provide a reasonable prediction for both the gross features and the detailed velocity field and turbulence-energy distribution in an inductively stirred system.

The principal discrepancy that one should expect would lie in the near-wall regions. Should one require more precise information regarding the behaviour of these regions, such as the knowledge of local heat- or mass-transfer rates, then the best alternative would be to measure these quantities directly. Work of this type is in progress in the author's laboratory at present.

The authors wish to thank Dr D. J. Moore and Dr J. C. R. Hunt of Cambridge University for helpful discussions and for providing us with experimental measurements. Thanks are also due to the National Aeronautics and Space Administration for the financial support of this work under Grant NSG 7645.

REFERENCES

GOSMAN, A. D., PUN, W. M., RUNCHAL, A. K., SPALDING, D. B. & WOLFSHTEIN, M. 1969 *Heat and Mass Transfer in Recirculating Flow*. Academic.

HUGHES, W. F. & YOUNG, F. J. 1966 *The Electromagnetodynamics of Fluids*. Wiley.

JACKSON, J. D. 1962 *Classical Electrodynamics*. Wiley.

KHALETZKY, D. 1976 Thesis, Université de Grenoble, France.

LAUNDER, B. E. & SPALDING, D. B. 1972 *Mathematical Models of Turbulence*. Academic.

LAUNDER, B. E. 1976 In *Heat and Mass Transport in Turbulence* (ed. P. Bradshaw), p. 232. Springer.

LAUNDER, B. E. & SPALDING, D. B. 1974 *Computer Meth. Appl. Mech. Engng* **3**, 269.

MOORE, D. J. 1982 Ph.D. thesis, Cambridge University.

MOORE, D. J. & HUNT, J. C. R. 1982*a* In *Proc.* 1981 *Electricity Counc. Res. Centre Seminar on Metal Flow in Induction Melting Furnaces* (ed. D. C. Lillicrap). *Electricity Res. Counc. Rep.* ERC/M1545.

MOORE, D. J. & HUNT, J. C. R. 1982*b* In *Proc. 3rd Beer-Sheva Seminar on Liquid Metal Flows and Magnetohydrodynamics. Prog. Astro. Aero.* **84**, AIAA.

NAKANISHI, K., SZEKELY, J., FUJII, T. & MIHARA, Y. 1975 *Met. Trans.* **6B**, 111.

PANOFSKY, W. K. H. & PHILLIPS, M. 1955 *Classical Electricity and Magnetism*. Addison-Wesley.

SZEKELY, J. & CHANG, C. W. 1977*a* *Ironmaking & Steelmaking* **4**, 190.

SZEKELY, J. & CHANG, C. W. 1977*b* *Ironmaking & Steelmaking* **4**, 196.

SZEKELY, J. & NAKANISHI, K. 1975 *Met. Trans.* **6B**, 245.

TARAPORE, E. D. & EVANS, J. W. 1976 *Met. Trans.* **7B**, 343.

TARAPORE, E. D. & EVANS, J. W. 1977 *Met. Trans.* **8B**.